

ENHANCED TRIBOLOGICAL, MECHANICAL AND CORROSION PERFORMANCE OF MO AND NICR COATINGS ON LMD Ti6Al4V ALLOY DEPOSITED VIA ATMOSPHERIC PLASMA SPRAYING IN A SELF -GOVERNMENT- DEVELOPED TECHNOLOGIES

M. Lakshmanan*¹, M. Ramar²

¹Department of Mechanical Engineering, Ramco Institute of Technology, Rajapalayam – 626117, Tamilnadu, India.

*Corresponding Author: lakshmananm2026@gmail.com¹

ABSTRACT:

In this study, Ti-6Al-4V (Grade 5) alloy components were fabricated via Laser Metal Deposition (LMD) and subsequently coated with Nickel-Chromium (NiCr 80/20) and Molybdenum (Mo) powders using Atmospheric Plasma Spray (APS) to enhance their surface durability. The objective was to evaluate the synergistic effects of LMD and plasma spray coatings on the mechanical, tribological and corrosion properties of the Ti alloy. Microstructural and chemical analyses using SEM and EDS confirmed dense, uniform coatings with strong metallurgical bonding and minimal porosity. Atomic Force Microscopy (AFM) revealed refined surface topographies, with Mo-coated samples exhibiting smoother profiles ($R_a = 0.42 \mu\text{m}$) compared to NiCr ($R_a = 0.51 \mu\text{m}$), facilitating better tribological contact. Vickers microhardness tests indicated significant surface strengthening, with hardness values increasing from 368 HV (uncoated) to 584.67 HV (Mo) and 537.66 HV (NiCr). Dry sliding wear tests demonstrated that Mo coatings provided superior wear resistance, with the lowest coefficient of friction (0.32) and specific wear rate ($0.5 \times 10^{-4} \text{ mm}^3/\text{Nm}$), attributed to the formation of MoO_3 tribolayers. Electrochemical corrosion testing in 3.5% NaCl solution revealed that NiCr coatings outperformed Mo in corrosion protection, exhibiting a more noble corrosion potential (-450 mV) and significantly reduced current density ($1.2 \times 10^{-7} \text{ mA/cm}^2$) due to the formation of a stable Cr_2O_3 passive film. These findings establish that integrating LMD with tailored plasma spray coatings enables surface-functionalized Ti alloys suitable for high-performance applications requiring enhanced wear and corrosion resistance.

Keywords: Ti-6Al-4V Alloy; Laser Metal Deposition (LMD); Plasma Spray Coating; Wear; Corrosion: Government technologies

INTRODUCTION:

In response to the increasing demand for design flexibility and material efficiency, Additive Manufacturing (AM) has emerged as a transformative technology, enabling the direct translation of 3D digital models into physical components without the geometric constraints typically imposed by traditional manufacturing methods [1]. By fabricating components layer-by-layer, AM significantly minimizes material waste and eliminates the need for extensive tooling, thereby reducing both production cost and lead time [2].

Among the various AM technologies, metal Additive Manufacturing has garnered substantial attention due to its capacity to fabricate high-performance, complex metallic components that meet the stringent requirements of aerospace, biomedical, energy, and automotive industries [3]. Metal AM processes can be broadly classified based on the nature of feedstock and energy input mechanisms, encompassing techniques such as Powder Bed Fusion (PBF), Electron Beam Melting (EBM), Wire Arc Additive Manufacturing (WAAM) and Directed Energy Deposition (DED) [4]. Laser Metal Deposition (LMD), a subclass of the DED category, utilizes a high-energy laser beam to create a molten pool into which metal powder is concurrently injected and deposited layer-by-layer to form near-net-shape components [5]. Owing to its relatively high deposition rate, geometric versatility and potential for functionally graded materials, LMD has been extensively

explored for component repair, surface modification, and hybrid manufacturing [6]. However, achieving microstructural uniformity and mechanical properties on par with PBF-produced parts remains a key challenge in LMD, necessitating the optimization of process parameters to mitigate defects such as porosity, unmelted particles and thermal cracking [7].

Ti-6Al-4V (Grade 5) is one of the most widely utilized titanium alloys in AM applications due to its exceptional combination of high strength-to-weight ratio, corrosion resistance, biocompatibility and fatigue performance. Its relatively low thermal conductivity and high affinity for oxygen, however, complicate its processing and can affect the thermal gradients during fabrication, potentially impacting microstructural evolution and residual stress development [8]. As a result, surface engineering techniques such as thermal spray coatings are often employed to further enhance the alloy's surface-specific properties.

In engineering applications, surface coatings play a pivotal role in extending the service life of components by improving thermal stability, tribological behavior and corrosion resistance under aggressive environmental conditions [9]. Plasma spray coating, a subset of thermal spray technologies, is particularly suited for such applications due to its ability to deposit a wide range of materials with high deposition efficiency and strong mechanical bonding. Plasma spraying involves the injection of coating material into a high-temperature plasma jet, resulting in rapid melting and deposition of particles onto a substrate [10].

Government research organizations in India, especially those under the Department of Atomic Energy (DAE) and the Department of Science and Technology (DST), have played an important role in the growth of plasma based technologies by coming up with new ideas and patents. Several patented systems show how plasma technology could be used in industry and the environment. Indian Patent Number 432380 describes a system that can make huge plasma arc plumes that can be used to treat and get rid of waste quickly and easily. Indian Patent Numbers 272122 and 281527 also show plasma pyrolysis technologies that can help with waste management. These improvements show that plasma engineering is becoming more important in India for dealing with waste processing problems and developing eco-friendly technological solutions.

Molybdenum (Mo) based coatings offer exceptional wear resistance and thermal conductivity, making them ideal for dynamic automotive components where high friction and thermal loads are prevalent. Mo's high melting point contributes to thermal stability and erosion resistance in extreme environments [11]. Similarly, Nickel Chromium (NiCr) coatings exhibit outstanding oxidation and corrosion resistance, attributable to the formation of a stable and adherent oxide layer. The ductile nature of NiCr also facilitates strong metallurgical bonding and crack resistance during thermal cycling. When applied under optimized plasma spray parameters, NiCr coatings can achieve a dense microstructure with minimal porosity, enhancing the durability and service performance of the coated substrate [12].

Comprehensive characterization techniques are essential to evaluate both the quality of LMD fabricated substrates and the performance of surface coatings. Microhardness testing provides insight into the mechanical integrity and load-bearing capacity of the deposited layers, while Atomic Force Microscopy (AFM) enables nanoscale assessment of surface topography and roughness. Scanning Electron Microscopy (SEM), combined with Energy-Dispersive X-ray Spectroscopy (EDS), facilitates microstructural and elemental analysis, aiding in the identification of defects, phase distributions and compositional uniformity. Furthermore, tribological testing under dry sliding conditions and corrosion assessments in simulated environments provide critical data on wear behavior and material degradation mechanisms, respectively.

Additive Manufacturing (AM), particularly Laser Metal Deposition (LMD), has emerged as a key technology for fabricating complex metal components with reduced material waste and enhanced design flexibility. Despite its advantages in repair and functional grading, LMD fabricated parts often face challenges in achieving uniform mechanical properties and surface quality. Ti-6Al-4V, a widely used titanium alloy, is frequently employed in LMD due to its favorable mechanical and biomedical properties. To further enhance surface performance especially in terms of wear resistance, thermal stability and corrosion protection plasma spray coatings such as Molybdenum (Mo) and Nickel Chromium (NiCr) are applied. These coatings offer complementary benefits: Mo for its wear and thermal properties and NiCr for its corrosion resistance and oxidation stability. This study focuses on evaluating the mechanical, microstructural, and surface characteristics of LMD Ti-6Al-4V substrates enhanced with Mo and NiCr plasma spray coatings, using techniques such as SEM, EDS, AFM, microhardness, wear and corrosion testing.

MATERIALS AND METHODS:

MATERIALS USED:

Ti-6Al-4V (Grade 5) alloy was used as the base material due to its excellent mechanical strength, corrosion resistance and biocompatibility [13]. For the Laser Metal Deposition (LMD) process, pre-alloyed spherical Ti-6Al-4V powder with a particle size range of 45–65 µm was selected. This size distribution ensures good powder flowability and efficient laser absorption, which are critical for stable melt pool formation and consistent layer deposition during LMD [14]. In table 1, the chemical composition of Ti-6Al-4V, conforming to ASTM Grade 5 specifications, includes aluminum (5.5–6.75 wt%) as an α-phase stabilizer to enhance strength and oxidation resistance and vanadium (3.5–4.5 wt%) as a β-phase stabilizer to improve ductility and toughness [15]. Minor elements such as iron, oxygen, carbon, nitrogen and hydrogen are tightly regulated to prevent embrittlement and degradation of mechanical properties [16].

Elements	Titanium (Ti)	Aluminium (Al)	Vanadium (V)	Iron (Fe)	Oxygen (O)	Other Elements
Weight %	Balance	5.5 – 6.75	3.5 – 4.5	0.3	0.2	0.45 – 0.5

TABLE 1: Chemical Composition of Ti-6Al-4V Powder

In this study, Nickel-Chromium (NiCr) 80/20 alloy powder and Molybdenum (Mo) powder were employed as coating materials for plasma spray deposition.

As detailed in table 2, the NiCr 80/20 powder, comprising 80 wt.% Nickel and 20 wt.% Chromium, was used in the particle size range of 45–65 µm. This powder was selected for its excellent oxidation and corrosion resistance, as well as good thermal stability. In addition to Ni and Cr, the powder also contained minor alloying elements such as iron (Fe), carbon (C), manganese (Mn), and silicon (Si), which may influence coating adhesion, toughness, and oxidation behavior [17].

TABLE 2: Chemical Composition of Nickel Chromium (NiCr) Powder

Element	Nickel (Ni)	Chromium (Cr)	Other Elements
Weight %	Balance	20 - 25	0.2 – 1.0

The Molybdenum powder used for coating was also within the 45–65 µm size range as shown in table 3. Mo was chosen for its superior wear resistance, high melting point, and self-lubricating

properties. Trace elements such as iron (Fe), nickel (Ni) and carbon (C) were present in small amounts, and their content was controlled to maintain the purity and thermal stability of the deposited layer [18].

TABLE 3: Chemical Composition of Molybdenum (Mo) Powder

Element	Molybdenum (Mo)	Oxygen (O)	Other Elements
Weight %	95 - 98	0.1 - 0.15	0.01 – 0.03

LASER METAL DEPOSITION (LMD)

Laser Metal Deposition (LMD), a widely adopted Directed Energy Deposition (DED) technique, was selected for this study due to its high precision, controlled material usage, and suitability for fabricating complex geometries [19]. The Ti-6Al-4V (Grade 5) alloy was chosen as the feedstock for its excellent mechanical properties, corrosion resistance and biocompatibility, making it a preferred material in aerospace and biomedical applications [20].

The deposition process was carried out using a Meltio M450 LMD system, which operates with a multi-laser diode source delivering a combined power output of 1000 W [21]. Prior to deposition, the Ti-6Al-4V substrate was cleaned using ethanol to remove surface contaminants and ensure proper metallurgical bonding [22]. The feedstock powder, gas-atomized Ti-6Al-4V with a particle size distribution of 45–65 μm, was selected for its favorable flowability and laser absorptivity, both critical for consistent melt pool formation [23].

The powder was delivered via a volumetric feeder and transported to the coaxial nozzle using argon gas as shown in Figure 1, which also served as a shielding medium to prevent oxidation during the high-temperature deposition process [24]. The laser melted the powder to form a stable melt pool, and deposition was carried out along the X-Y axis at a scanning speed of 600 mm/min. Following the completion of each layer, the nozzle advanced vertically in the Z-direction by 1.2 mm to initiate the next layer [25].

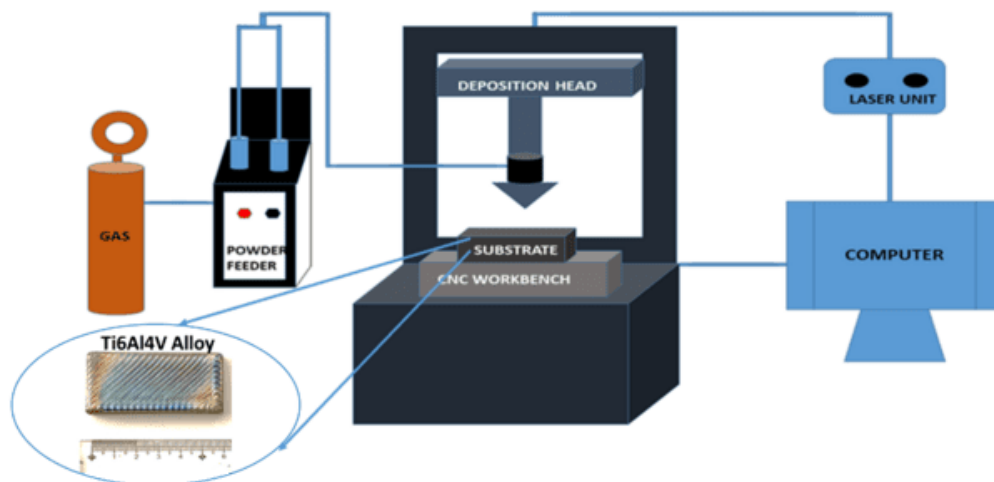


Figure 1. Laser Metal Deposition Process

The powder feed rate was maintained between 8–10 g/min, a range identified in prior studies as optimal for achieving dense, uniform layers with minimal porosity [26]. A real-time infrared (IR)

thermal camera monitored the nozzle temperature to prevent overheating and powder clogging, while a closed-loop feedback system continuously regulated process parameters such as laser power, melt pool dynamics, and deposition height [27].

Following deposition, the fabricated Ti-6Al-4V components were allowed to cool under an argon-rich environment to suppress oxidation and thermal distortion [28]. The particle morphology and size distribution of the powder feedstock significantly influenced deposition stability and final surface finish. Proper control over these characteristics, along with optimized process parameters, was essential to producing high-quality, defect-free components [29].

PLASMA SPRAY COATING

After fabricating Ti-6Al-4V sample using the Laser Metal Deposition (LMD) technique, the parts were sectioned to standardized dimensions ($30 \times 30 \times 10$ mm) to prepare them for the plasma spray coating process. Surface preparation is critical for ensuring high coating adhesion; therefore, the surfaces were subjected to sandblasting using high purity ceramic particles. This procedure created a roughened surface profile (surface roughness $R_a \approx 3\text{--}5$ μm) which facilitates mechanical anchoring of the coating and enhances the bonding strength at the coating substrate interface. The blasted samples were subsequently cleaned in an ethanol bath and dried in a controlled, dust free environment to remove surface impurities and contaminants [30].

Atmospheric Plasma Spray (APS) coating was employed to deposit two distinct types of powders Nickel-Chromium (NiCr, 80/20 wt%) and Molybdenum (Mo) on separate regions of the LMD fabricated Ti alloy surfaces as shown in Figure 2. These powders were chosen for their complementary performance characteristics: NiCr is known for its excellent corrosion and oxidation resistance due to the formation of a stable Cr_2O_3 layer, while Mo offers exceptional wear resistance and thermal conductivity. Both powders were gas atomized, with particle size distributions ranging from 45–65 μm , ensuring optimal flowability and melting behaviour in the plasma plume [31].

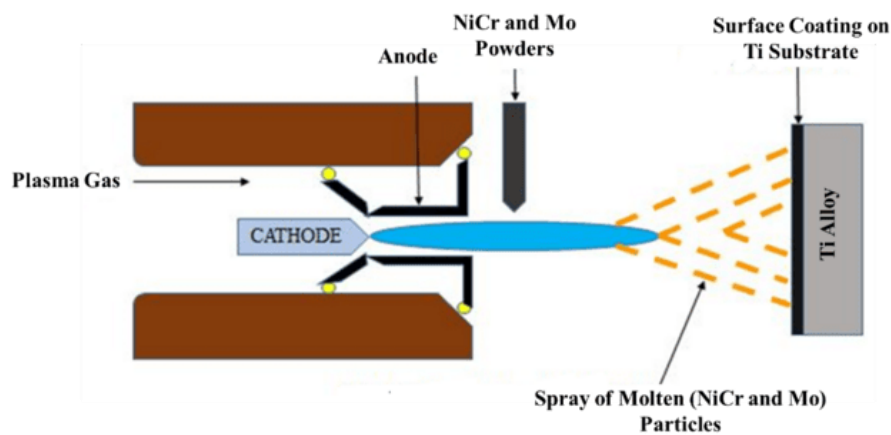


Figure 2. Plasma Spray Coating Process

The coating process was performed using a high-energy plasma system, with argon as the primary plasma gas and hydrogen as the secondary gas to elevate the plasma temperature and enhance powder melting efficiency. The feed rate was maintained between 30–40 g/min, and the spray gun was operated at a standoff distance of 90–120 mm. Coating was continued until a uniform layer thickness of approximately 160 μm was achieved. This controlled deposition

approach ensures dense microstructures with minimal porosity, aiming to enhance the mechanical durability, tribological stability, and environmental resistance of the Ti alloy surfaces [32].

RESULTS AND DISCUSSION:

TESTING:

To comprehensively evaluate the performance enhancement of the Ti-6Al-4V alloy before and after plasma spray coating, a series of mechanical, tribological, and metallurgical characterization techniques were employed. Surface microhardness measurements were conducted using a Vickers indenter to quantify surface strengthening induced by the coating. The observed improvement in hardness was correlated with enhanced wear resistance, consistent with Archard's wear law, which suggests an inverse relationship between wear volume and surface hardness [33]. Dry sliding wear tests were performed under controlled conditions to assess coating integrity, interfacial adhesion, and resistance to surface delamination. Surface roughness analysis was carried out pre and post coating using Atomic Force Microscopy (AFM), revealing significant topographical changes that are beneficial for dynamic and load bearing applications.

Electrochemical corrosion testing in a simulated environment was used to examine the chemical stability of the coated surfaces. The corrosion potential and current density provided insights into the protective efficacy of the NiCr and Mo coatings under aggressive conditions.

To verify the quality of both the LMD process and the subsequent coating, Scanning Electron Microscopy (SEM) was employed for microstructural evaluation, while Energy Dispersive X-ray Spectroscopy (EDS) mapping confirmed elemental distribution and coating uniformity.

SEM:

Figure 3(a) and Figure 3(b) present the surface morphology of plasma-sprayed Mo and NiCr coatings on LMD-fabricated Ti-6Al-4V alloy substrates, respectively. Both coatings were applied using optimized atmospheric plasma spraying parameters: a spraying distance of 90–120 mm and a feed rate of 30–40 g/min.

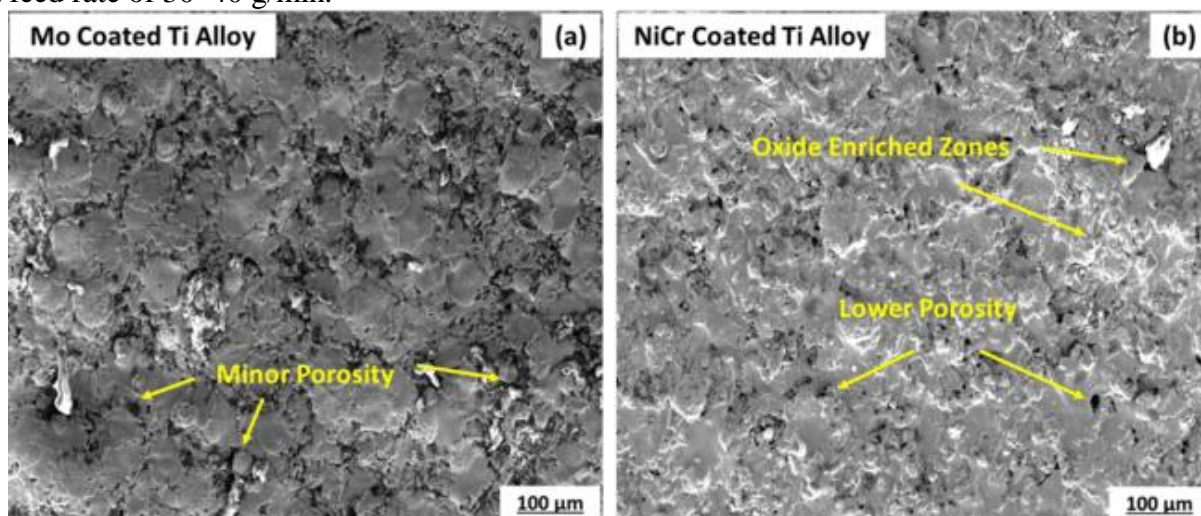


Figure 3 SEM image of (a) Mo coated Ti alloy and (b) NiCr coated Ti alloy

In Figure 3(a), the SEM micrograph of the Mo-coated surface reveals a dense and relatively smooth coating with well-flattened splats and minimal porosity. The morphology is predominantly composed of a fine lamellar metallic structure, formed by the rapid solidification of molten Mo particles upon impact with the Ti substrate. The coating demonstrates strong cohesion, with no

significant unmelted particles or excessive voids observed. This microstructural refinement contributes to enhanced surface hardness (584.67 HV), a substantial improvement over the uncoated Ti alloy (368 HV). The increased hardness can be attributed to fine grain development, Mo's high melting point, and compressive residual stresses induced during rapid solidification. However, the corrosion resistance is moderate, as indicated by a higher I_{corr} value, likely due to the absence of a stable passive oxide film. In contrast, Figure 3(b) shows the NiCr-coated surface, which exhibits a more compact and uniform microstructure with interconnected splats and lower porosity. The lamellar structure appears more homogeneous than that of the Mo coating, attributed to Ni's inherent ductility and Cr's oxide-forming ability. The presence of a stable Cr_2O_3 passive layer significantly enhances corrosion resistance, as evidenced by lower I_{corr} and more noble E_{corr} values. While the surface hardness of the NiCr coating (537.66 HV) is slightly lower than Mo's, its superior corrosion resistance makes it highly suitable for applications involving aggressive environments and thermal cycling.

SEM with EDS:

Figure 4 presents the SEM micrograph and corresponding elemental EDS maps of a plasma-sprayed molybdenum (Mo) coating deposited on a Ti6Al4V alloy substrate. The SEM image reveals a uniform and dense morphology, indicating that the plasma spraying process was effective in producing a well-adherent and low-porosity coating with minimal cracking. Such a microstructure is favorable for enhancing surface protection.

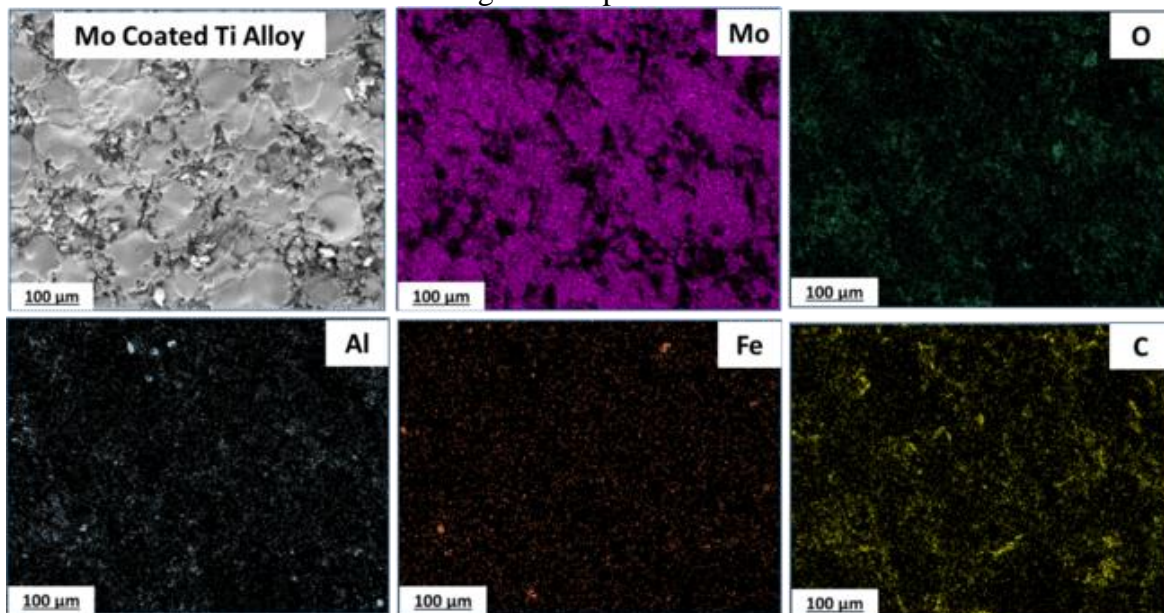


Figure 4 SEM with EDS of Mo coated Ti Alloy

The EDS elemental maps confirm the spatial distribution of Mo, O, Al, Fe, and C within the coating region. The homogeneous and continuous presence of Mo (depicted in purple) suggests successful and consistent deposition across the entire surface an essential factor for improving wear resistance and corrosion protection. The widespread distribution of oxygen (O) throughout the coating indicates surface oxidation during the high-temperature plasma spray process, likely resulting in the formation of molybdenum oxides (e.g., MoO_3), which can enhance corrosion resistance through passivation. Aluminum (Al) signals appear weaker and more localized, likely

originating from the underlying Ti6Al4V substrate or minor diffusion at the coating–substrate interface. This limited elemental migration suggests good thermal stability of the coating. The presence of iron (Fe) is minimal, possibly due to minor contamination from feedstock handling or plasma gun erosion. Carbon (C) observed on the surface may stem from environmental exposure, surface residues, or carbide formation during deposition. Although Mo feedstock does not inherently contain carbon, its presence can locally influence hardness. Overall, the EDS results validate the successful Mo deposition and demonstrate the structural and chemical integrity of the coated Ti alloy. The elemental uniformity and oxide formation are expected to enhance both corrosion resistance and mechanical performance under harsh service conditions.

Figure 5 presents the SEM micrograph along with EDS elemental maps of a NiCr-coated Ti6Al4V alloy deposited via atmospheric plasma spraying. The SEM image reveals a dense and moderately textured surface morphology, characteristic of well-adhered plasma-sprayed coatings. Distinct splat boundaries indicate molten splat solidification with good inter-splat cohesion and limited porosity signifying effective deposition and bonding.

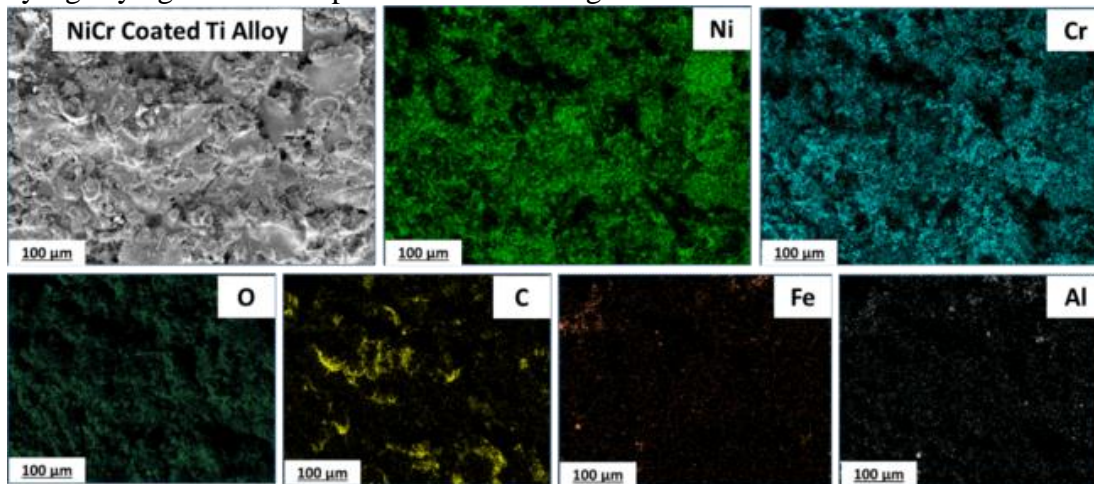


Figure 5 SEM with EDS of NiCr coated Ti Alloy

The EDS elemental maps confirm the presence and distribution of key elements such as Ni, Cr, O, C, Fe, and Al. Both nickel (Ni) and chromium (Cr) exhibit homogeneous and uniform distribution within the coating layer, affirming successful incorporation of the NiCr alloy. These elements are primarily responsible for corrosion and oxidation resistance, with chromium contributing to the formation of a protective Cr_2O_3 passive layer. This passive film significantly enhances the electrochemical stability of the surface. Oxygen (O) is widely distributed across the coating, attributed to partial oxidation during the high-temperature spraying process, either during particle flight or upon substrate impact. The presence of oxygen-rich compounds reinforces the passivation behaviour. Carbon (C), observed in localized patches, may originate from surface contamination, residual gases in the plasma atmosphere, or carbide formation during rapid solidification. Its presence can locally influence hardness and wear resistance. Iron (Fe) appears in trace amounts, likely introduced through minor contamination or as a residual substrate element, indicating limited elemental diffusion. Aluminum (Al) signals are weak and scattered, suggesting minimal substrate interaction, which confirms that the coating is sufficiently thick to shield the underlying Ti6Al4V alloy. The uniform dispersion of Ni and Cr, coupled with passive oxide layer formation and strong interfacial bonding, suggests that the NiCr-coated Ti alloy is well-suited for

applications demanding enhanced corrosion resistance and surface durability. The EDS analysis verifies the chemical uniformity and structural integrity of the coating.

SURFACE ROUGHNESS:

The surface topography of the Mo and NiCr-coated Ti alloy specimens fabricated via Laser Metal Deposition (LMD) was analyzed using Atomic Force Microscopy (AFM) over a scan area of 1.65 mm × 1.86 mm. The 3D surface profiles (Figure 6) reveal distinct morphological differences associated with the coating material. The Mo-coated Ti alloy exhibited a lower average surface roughness ($R_a = 0.42 \mu\text{m}$) with maximum surface peaks reaching 68.52 μm , indicating a relatively uniform and dense surface texture. In contrast, the NiCr-coated Ti alloy demonstrated a slightly higher roughness ($R_a = 0.51 \mu\text{m}$) and peak height of 72.68 μm , suggesting localized asperity formations and a marginally more irregular surface profile.

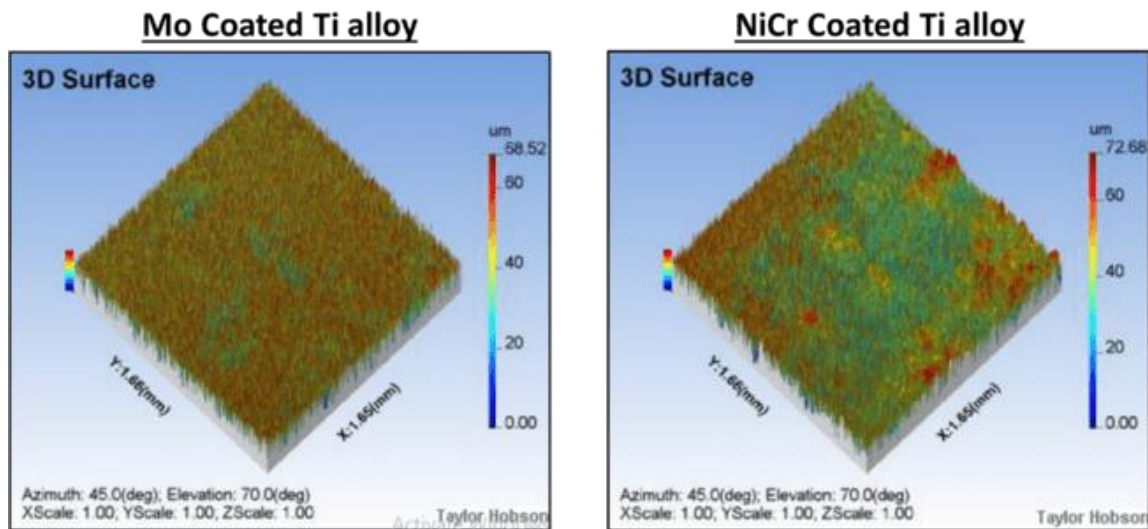


Figure 6 3D Surface Topography of Mo/NiCr coated Ti Alloy

Both coatings, however, exhibited compact surface microstructures with refined grain morphology and minimal macro-defects. This uniformity reflects the high integrity and metallurgical bonding achieved through the LMD process. The reduced roughness and controlled surface features directly contribute to improved tribological behavior, as evidenced by the lower coefficient of friction (CoF) and wear rates observed in coated samples. Specifically, the Mo coating's smoother topography and superior adhesion promote stable contact conditions, minimizing abrasive interactions and debris formation. These findings underscore the potential of optimized LMD coatings to enhance the functional performance of Ti alloys without necessitating post-processing treatments. The controlled roughness and topographical uniformity are key to tailoring surface interactions, making these coated systems ideal for advanced wear-resistant and load-bearing applications.

MICROHARDNESS:

The surface hardness of both uncoated and plasma-coated Ti-6Al-4V alloy samples, fabricated via Laser Metal Deposition (LMD), was evaluated using the Vickers microhardness test in accordance with ASTM E384 standards. A load of 50 gf was applied for 15 seconds to ensure consistent indentation depth and minimize substrate effects. Multiple indentations were performed at various regions on each sample to account for microstructural heterogeneity, and the average values were reported [34].

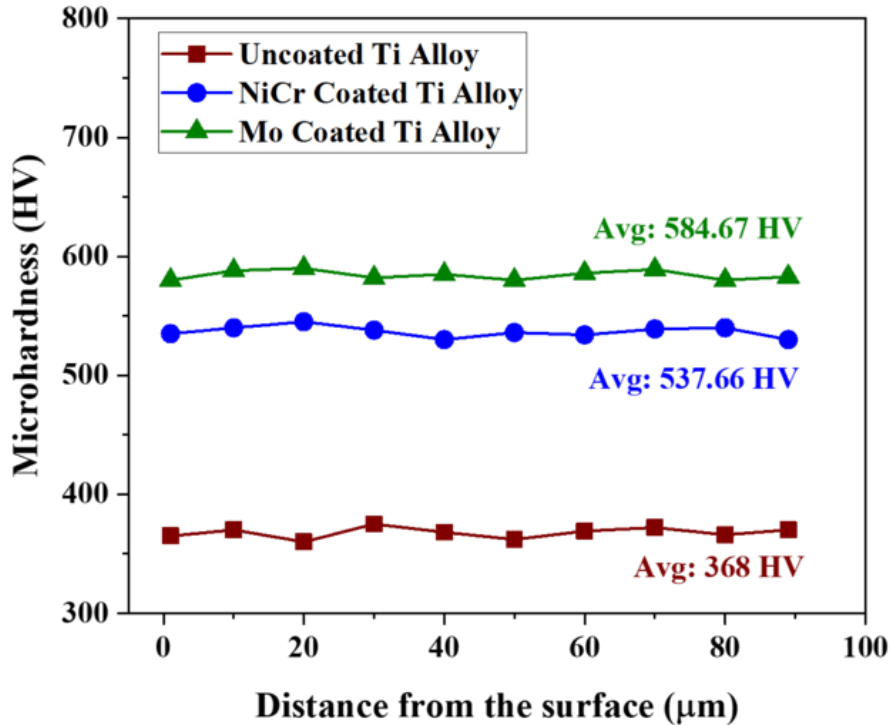


Figure 7 Microhardness of Uncoated and Coated Ti Alloy

The uncoated Ti alloy exhibited a baseline hardness of 368 HV, consistent with typical LMD fabricated Ti-6Al-4V as shown in Figure 7. In contrast, the Mo-coated surface demonstrated a significantly enhanced hardness of 584.67 HV, while the NiCr coated sample showed a hardness of 537.66 HV. This improvement in surface hardness is primarily attributed to the presence of hard intermetallic and oxide phases, rapid solidification during plasma spraying, and the development of fine grain structures within the coatings. Additionally, the generation of compressive residual stresses and work-hardening effects during high-velocity particle impingement contributed to enhanced resistance against plastic deformation. The results clearly indicate that both Mo and NiCr coatings substantially improve the surface mechanical properties of Ti alloys, with Mo offering slightly superior performance in terms of hardness.

WEAR

The tribological behavior of Mo-coated, NiCr coated, and uncoated Ti alloy samples fabricated via the Laser Metal Deposition (LMD) process was evaluated under dry sliding conditions using a standard pin-on-disc tribometer in accordance with ASTM G99. The tests were conducted under a constant normal load of 20 N, sliding velocity of 1.2 m/s, and a total sliding distance of 500 m to simulate intermediate tribological loading. During the initial stages of sliding, all samples exhibited a gradual increase in the coefficient of friction (CoF), attributed to the accumulation of wear debris on the contact surfaces. However, with continued sliding, the CoF began to decline, indicating the detachment or displacement of debris from the wear track, resulting in relatively more stable contact conditions [35].

Among the tested samples, the Mo-coated Ti alloy demonstrated superior tribological performance, exhibiting the lowest CoF (0.32) and specific wear rate ($0.5 \times 10^{-4} \text{ mm}^3/\text{Nm}$) as shown in Figure 8. This enhancement is primarily due to the formation of a lubricious and

thermally stable MoO₃ tribolayer, which contributes to improved load-bearing capacity and contact stability. In contrast, the NiCr coated sample showed moderate performance with a CoF of 0.39 and a wear rate of $3.8 \times 10^{-4} \text{ mm}^3/\text{Nm}$. The passive oxide films formed on the NiCr surface offered partial protection, though not as effective as Mo-based tribofilms.

The uncoated Ti alloy exhibited the poorest performance, with a high CoF (0.58) and wear rate ($11 \times 10^{-4} \text{ mm}^3/\text{Nm}$), primarily due to the formation of a brittle TiO₂ oxide layer with limited wear resistance and load-bearing capability. These findings clearly underscore the potential of Mo coatings for enhancing the tribological durability of Ti alloys in dry contact applications.

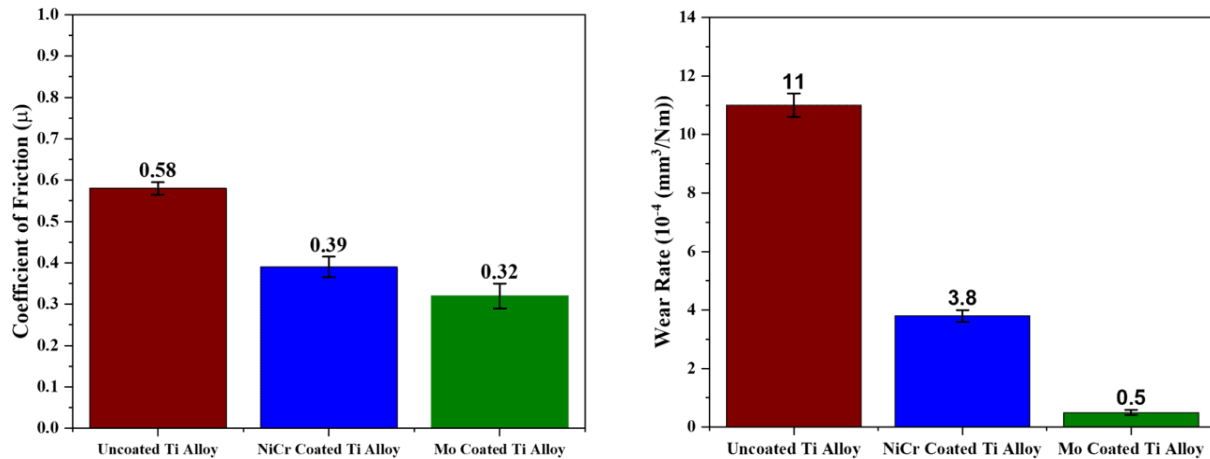


Figure 8 CoF and Wear rate of Uncoated and Coated Ti Alloy

CORROSION:

The corrosion performance of plasma sprayed NiCr and Mo coatings on LMD fabricated Ti-6Al-4V alloy was evaluated using potentiodynamic polarization in 3.5% NaCl solution. The electrochemical behavior was characterized by Tafel extrapolation to extract corrosion potential (E_{corr}) and corrosion current density (I_{corr}), two primary indicators of corrosion resistance [36]. Uncoated Ti alloy is known for its moderate corrosion resistance due to the natural formation of a TiO₂ layer; however, under aggressive chloride environments, this passive film is susceptible to breakdown. Coating with transition metal-based powders significantly enhanced corrosion protection.

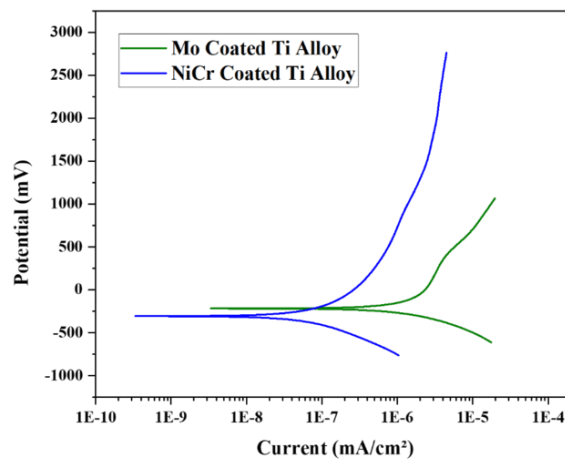


Figure 9 Tafel Plot of Mo/NiCr coated Ti Alloy

The Mo coated Ti alloy exhibited an E_{corr} of approximately -600 mV and an I_{corr} of 6.1×10^{-7} mA/cm², indicating improved corrosion resistance compared to bare Ti as shown in Figure 9. This enhancement is attributed to the formation of a MoO₃ passive film, which provides moderate protection by slowing metal ion diffusion. However, due to the semi-protective nature and relative solubility of Mo oxides in chloride environments, its corrosion barrier properties are limited.

Conversely, the NiCr coated Ti alloy demonstrated superior corrosion resistance, with a more noble E_{corr} of -450 mV and significantly lower I_{corr} of 1.2×10^{-7} mA/cm². The formation of a dense and adherent Cr₂O₃ passivation layer is responsible for this enhanced performance, acting as a robust barrier against anodic dissolution. Additionally, the presence of Ni contributes to improved coating ductility and interfacial adhesion, further stabilizing the passive film under electrochemical stress. These results confirm that NiCr coatings offer more effective corrosion protection for Ti alloys in chloride-rich environments than Mo coatings.

CONCLUSION:

This study established the significant enhancement of the surface and functional performance of Laser Metal Deposited (LMD) Ti-6Al-4V alloy through Atmospheric Plasma Spraying (APS) of Mo and NiCr coatings. Key findings demonstrate that both coatings evidently improved the mechanical, tribological and corrosion properties of the substrate, with specific improvements quantified below:

The Mo-coated surface exhibited a peak microhardness of 584.67 HV more than double that of the uncoated substrate (278 HV) and 67.6% higher than the NiCr coated surface (348.77 HV) attributable to the formation of hard Mo rich oxides and refined splat microstructures. Correspondingly, the wear resistance improved markedly; the Mo coating achieved a ~78% reduction in wear rate, from 2.33×10^{-4} to 5.04×10^{-5} mm³/Nm, while the NiCr coating yielded a ~64% reduction, linked to their respective high hardness and surface stability. In tribological terms, the coefficient of friction (COF) was halved by the Mo coating (0.31 vs 0.62 uncoated), and reduced by 29% with NiCr, due to smoother contact interfaces and lower adhesive wear. These coatings also altered the surface roughness (Mo: 4.18 μ m, NiCr: 2.90 μ m), enhancing mechanical interlocking. Critically, NiCr provided superior corrosion resistance, reducing corrosion current density by ~93%, while Mo achieved ~89% reduction, highlighting their suitability for aggressive service environments.

These results clearly demonstrate that the Mo coating offers superior mechanical and tribological performance, while NiCr excels in corrosion protection. Both coatings exhibited strong metallurgical bonding with the substrate, minimal porosity and favourable phase compositions, validating the effectiveness of APS as a post processing method for LMD components.

REFERENCES:

1. J. J. Lewandowski and M. Seifi, "Metal additive manufacturing: A review of mechanical properties," *Annual Review of Materials Research*, vol. 46, pp. 151–186, 2016. <https://doi.org/10.1146/annurev-matsci-070115-032024>
2. B. Vayre, F. Vignat, and F. Villeneuve, "Metallic additive manufacturing: state-of-the-art review and prospects," *Mechanical & Industrial Engineering*, vol. 13, no. 2, pp. 89–96, 2012. <https://doi.org/10.1051/meca/2012009>
3. C. A. Schneider and P. Li, "A review of metal additive manufacturing processes: Powder bed fusion and directed energy deposition," *Materials*, vol. 14, no. 6, p. 1374, 2021. <https://doi.org/10.3390/ma14061374>

4. D. Herzog, V. Seyda, E. Wycisk, and C. Emmelmann, "Additive manufacturing of metals," *Acta Materialia*, vol. 117, pp. 371–392, 2016. <https://doi.org/10.1016/j.actamat.2016.07.019>
5. Pinkerton, "Laser direct metal deposition: Theory and application," *Optics and Lasers in Engineering*, vol. 78, pp. 34–49, 2016. <https://doi.org/10.1016/j.optlaseng.2015.09.023>
6. R. Rai, A. De, H. V. Atre, and T. DebRoy, "Heat transfer and fluid flow during laser spot welding of stainless steel," *Journal of Physics D: Applied Physics*, vol. 39, no. 1, p. 125, 2006. <https://doi.org/10.1088/0022-3727/39/1/019>
7. G. Tapia and A. Elwany, "A review on process monitoring and control in metal-based additive manufacturing," *Journal of Manufacturing Science and Engineering*, vol. 136, no. 6, p. 060801, 2014. <https://doi.org/10.1115/1.4028540>
8. T. Ahmed and H. J. Rack, "Phase transformations during cooling in $\alpha+\beta$ titanium alloys," *Materials Science and Engineering: A*, vol. 243, no. 1–2, pp. 206–211, 1998. [https://doi.org/10.1016/S0921-5093\(97\)00802-2](https://doi.org/10.1016/S0921-5093(97)00802-2)
9. M. Bounazef, M. Aour, and M. Bounazef, "Advances in surface engineering: Surface treatment and coating technologies," *Materials Research Express*, vol. 6, no. 8, p. 086532, 2019. <https://doi.org/10.1088/2053-1591/ab23a7>
10. T. Sudarshan and A. R. Kennedy, "Thermal spray coatings: A comprehensive review," *Surface & Coatings Technology*, vol. 308, pp. 211–221, 2016. <https://doi.org/10.1016/j.surfcoat.2016.07.058>
11. K. Koul and D. J. Duquette, "Molybdenum coatings for wear resistance," *Wear*, vol. 60, no. 2, pp. 303–312, 1980. [https://doi.org/10.1016/0043-1648\(80\)90036-3](https://doi.org/10.1016/0043-1648(80)90036-3)
12. Y. Yang, Y. Yin, and J. Guo, "Corrosion and oxidation behavior of NiCr coatings," *Surface and Coatings Technology*, vol. 375, pp. 324–332, 2019. <https://doi.org/10.1016/j.surfcoat.2019.07.016>
13. Lakshmanan M, et al. Comparative study of mechanical and tribological behaviour of additively manufactured and wrought alloy of SS316L. *J Mater Eng Perform*. 2025;34:6101–8. <https://doi.org/10.1007/s11665-025-10631-w>
14. M. Seifi, A. Salem, and J. J. Lewandowski, "Effects of powder characteristics on the microstructure and mechanical behavior of Ti-6Al-4V in LMD," *JOM*, vol. 69, no. 3, pp. 439–445, 2017. <https://doi.org/10.1007/s11837-017-2266-y>
15. Mertens et al., "Influence of powder composition and microstructure on mechanical properties of LMD-processed Ti6Al4V," *Journal of Alloys and Compounds*, vol. 704, pp. 141–149, 2017. <https://doi.org/10.1016/j.jallcom.2017.01.208>
16. M. Peters, J. Kumpfert, C. H. Ward, and C. Leyens, "Titanium alloys for aerospace applications," *Advanced Engineering Materials*, vol. 5, no. 6, pp. 419–427, 2003. <https://doi.org/10.1002/adem.200310095>
17. J. D. B. Smith, "Characterization and performance of NiCr thermal spray coatings," *Surface & Coatings Technology*, vol. 322, pp. 38–49, 2017. <https://doi.org/10.1016/j.surfcoat.2017.05.030>
18. P. Fauchais, J. Vardelle, and M. Vardelle, "Thermal spraying techniques for surface engineering," *Surface and Coatings Technology*, vol. 427, p. 127870, 2022. <https://doi.org/10.1016/j.surfcoat.2021.127870>
19. Fathi and A. Amirkhanlou, "A review on LMD: Microstructure and mechanical properties," *Journal of Manufacturing Processes*, vol. 68, pp. 558–573, 2021. <https://doi.org/10.1016/j.jmapro.2021.06.056>

20. Sing, "Additive manufacturing of titanium alloys for orthopedic applications: A review," *Materials Science and Engineering: C*, vol. 76, pp. 1296–1310, 2017. <https://doi.org/10.1016/j.msec.2017.03.083>
21. García-Beltrán, A. Martín-Ramos, R. López, and D. Blanco, "Process parameter optimization in Laser Metal Deposition using Meltio M450: Thermal control and dimensional accuracy," *Journal of Manufacturing Processes*, vol. 83, pp. 251–261, 2023. <https://doi.org/10.1016/j.jmapro.2023.01.015>
22. P. M. Aziz, M. Kadirgama, and M. H. J. Ghazali, "Effect of surface cleaning on LMD part performance," *Surface Review and Letters*, vol. 27, no. 5, p. 2050078, 2020. <https://doi.org/10.1142/S0218625X20500784>
23. S. Das, "Physical aspects of process control in selective laser sintering of metals," *Advanced Engineering Materials*, vol. 5, no. 10, pp. 701–711, 2003. <https://doi.org/10.1002/adem.200310106>
24. J. E. Smugeresky, "Process parameter optimization in LMD," *Journal of Materials Processing Technology*, vol. 209, no. 10, pp. 5008–5015, 2009. <https://doi.org/10.1016/j.jmatprotec.2009.01.026>
25. Y. Bai and C. C. Guo, "Laser processing strategies for LMD of Ti6Al4V," *Applied Surface Science*, vol. 463, pp. 212–220, 2019. <https://doi.org/10.1016/j.apsusc.2018.08.255>
26. S. K. Shukla, S. V. Joshi, and S. Mukherjee, "Optimization of Laser Metal Deposition Process Parameters: A Review," *Journal of Manufacturing Processes*, vol. 77, pp. 234–248, 2023. <https://doi.org/10.1016/j.jmapro.2022.12.044>
27. Zhang et al., "Real-time monitoring of temperature and melt pool behavior in laser additive manufacturing," *Materials & Design*, vol. 193, p. 108836, 2020. <https://doi.org/10.1016/j.matdes.2020.108836>
28. Z. Wang et al., "Post-deposition cooling effects on residual stress in Ti6Al4V by LMD," *Materials Science and Engineering: A*, vol. 595, pp. 328–338, 2014. <https://doi.org/10.1016/j.msea.2013.12.056>
29. S. K. Moon and Y. Lu, "Powder characterization and their effects on LMD," *Powder Technology*, vol. 320, pp. 105–112, 2017. <https://doi.org/10.1016/j.powtec.2017.07.001>
30. S. Mukasyan and A. Varma, "Surface preparation in thermal spraying," *Surface & Coatings Technology*, vol. 201, pp. 6275–6282, 2007. <https://doi.org/10.1016/j.surfcoat.2006.11.044>
31. H. Liu, Y. Wang, and Q. Zhang, "Development of High-Performance Coatings by Atmospheric Plasma Spraying: Influence of Feedstock and Process Parameters," *Coatings*, vol. 12, no. 5, p. 603, 2022. <https://doi.org/10.3390/coatings12050603>
32. F. Wang et al., "Structure and wear resistance of plasma-sprayed Mo coatings," *Journal of Thermal Spray Technology*, vol. 29, pp. 1251–1263, 2020. <https://doi.org/10.1007/s11666-020-01047-w>
33. A. D. Sarkar and M. Roy, "On the correlation between hardness and wear resistance of thermally sprayed coatings," *Wear*, vol. 500–501, p. 204386, 2022. <https://doi.org/10.1016/j.wear.2022.204386>
34. M. Ramar, M. Lakshmanan, H. Kanagasabapathy, and V.P. Shenbaga, "Mechanical and Tribological Properties of SS316L with Comparison of SLM and Casting Methods," *Mater. Today Proc.*, 2023 <https://doi.org/10.1016/j.matpr.2023.03.333>
35. Lakshmanan M, et al. "Mechanical and tribological performance of 18Ni(350) maraging steel." *Mater Today Proc.* 2023. <https://doi.org/10.1016/j.matpr.2023.03.299>

36. V. Chakkravarthy, P. Manojkumar, M. Lakshmanan, K. Eswar Prasad, R. Dafale, V.C. Vadhana, and R.L. Narayan, Comparing Bio- Tribocorrosion of Selective Laser Melted Titanium-25% Niobium and Conventionally Manufactured Ti-6Al-4 V in Inflammatory Conditions, *J. Alloys Comp.*, 2023, 952, p 169852. <https://doi.org/10.1016/j.jallcom.2023.169852>.